The crystal structure of pseudokinase PEAK1 (Sugen kinase 269) reveals an unusual catalytic cleft and a novel mode of kinase fold dimerization

Received for publication, November 1, 2017, and in revised form, November 30, 2017 Published, Papers in Press, December 6, 2017, DOI 10.1074/jbc.RA117.000751

Byung Hak Ha[‡] **and Titus J. Boggon**[‡§1]

From the Departments of [‡]*Pharmacology and* [§]*Molecular Biophysics and Biochemistry, Yale University, New Haven, Connecticut 06520*

Edited by Wolfgang Peti

The pseudokinase group encompasses some 10% of protein kinases, but pseudokinases diverge from canonical kinases in key motifs. The two members of the small new kinase family 3 (NKF3) group are considered pseudokinases. These proteins, pseudopodium-enriched atypical kinase 1 (PEAK1, Sugen kinase 269, or SgK269) and pragmin (Sugen kinase 223 or SgK223), act as scaffolds in growth factor signaling pathways, and both contain a kinase fold with degraded kinase motifs at their C termini. These kinases may harbor regions that mediate oligomerization or control other aspects of signal transduction, but a lack of structural information has precluded detailed investigations into their functional roles. In this study, we determined the X-ray crystal structure of the PEAK1 pseudokinase domain to 2.3 Å resolution. The structure revealed that the PEAK1 kinase-like domain contains a closed nucleotide-binding cleft that in this conformation may deleteriously affect nucleotide binding. Moreover, we found that N- and C-terminal extensions create a highly unusual all α-helical split-dimerization region, termed here the split helical dimerization (SHED) region. Sequence conservation analysis suggested that this region facilitates a dimerization mode that is conserved between PEAK1 and pragmin. Finally, we observed structural similarities between the PEAK1 SHED region and the C-terminal extension of the Parkinson's disease-associated kinase PINK1. In summary, PEAK1's kinase cleft is occluded, and its newly identified SHED region may promote an unexpected dimerization mode. Similarities of PEAK1 with the active kinase PINK1 may reclassify the latter as a member of the new kinase family 3 group.

Pseudopodium-enriched atypical kinase (PEAK1; Sugen kinase 269; SgK269)[2] is a large (1,746 amino acid) cytoplasmic protein that acts as a scaffold for growth factor signaling pathways (1–3). It is tyrosine-phosphorylated in response to growth factor activation which creates SH2 domain binding sites for Shc1-, Grb2-, Csk-, and Src-family kinases (4–11). Increased PEAK1 expression is associated with metastasis and proliferation of cancer cells, including in prostate, pancreatic, colon, and breast cancers (1, 4–7, 9, 12–15), and these changes are thought to correspond to altered temporal regulation of growth factor signaling via the PEAK1 phosphotyrosine–SH2 domain interactions (4, 10). These scaffolding functions of PEAK1 are consistent with a role for this protein as an oncogene (6); however, the phosphorylation sites occur in a predicted unstructured region distal to the PEAK1 C-terminal kinase-fold domain (Fig. 1*A*). The role of this kinase-like domain in signal transduction pathways and tumorigenesis remains unclear.

Pseudokinases encompass some 10% of the human kinome but diverge from canonical kinases in key catalytic motifs (16, 17). They are the quintessential pseudoenzymes, and like other nucleotide-binding pseudoenzymes, the pseudokinase family members are classified as either being catalytically active, being able to bind nucleotide but harboring no catalytic activity, or being unable to bind nucleotide (18–22). This diversity belies a wide range of functions for the pseudokinase group, from conventional transferase activity, to actions as binders and modifiers of signaling from typical kinases, to acting as scaffolds for signaling complexes (19). PEAK1 is divergent from canonical kinases in multiple of the conserved kinase motifs (the glycine-rich loop, the HRD motif, and the DFG motif) (Fig. 1*B*); consequently, it is classified as a pseudokinase. Subclassification of PEAK1 into one of the pseudokinase groups (ATP-binder/catalytically active, ATP-binder/catalytically inactive, or ATP-non-binder) has not been consistent (1, 5, 9, 23), but because of the divergence in ATP-binding cleft residues (Fig. 1*B*) and limited effect of nucleotide on PEAK1 denaturation (18), consensus has built to support the "unable to bind nucleotide" classification.

Sequence analysis has suggested that PEAK1 is a member of a small protein kinase family termed the new kinase family 3

This work was supported by National Institutes of Health Grants R01NS085078, R01GM109487, R01GM114621, R01GM102262, and S10OD018007. The authors declare that they have no conflicts of interest with the contents of this article. The content is solely the responsibility of the authors and does not necessarily represent the official views of the National Institutes of Health.

The atomic coordinates and structure factors (code 6BHC) have been deposited in the Protein Data Bank (http://wwpdb.org/).

X-ray diffraction images are available online at SBGrid Data Bank under 10.15785/SBGRID/514.

This article contains Fig. S1.

[1] To whom correspondence should be addressed: Depts. of Pharmacology and of Molecular Biophysics and Biochemistry, Yale University, SHM B-316A, 333 Cedar St., New Haven, CT 06520. Tel.: 203-785-2943; Fax: 203-785-5494; E-mail: titus.boggon@yale.edu.

[2] The abbreviations used are: PEAK, pseudopodium-enriched atypical kinase; RMSD, root mean square deviation; NKF, new kinase family; SgK, Sugen kinase; SHED, split helical dimerization; CTE, C-terminal extension; PDB, Protein Data Bank.

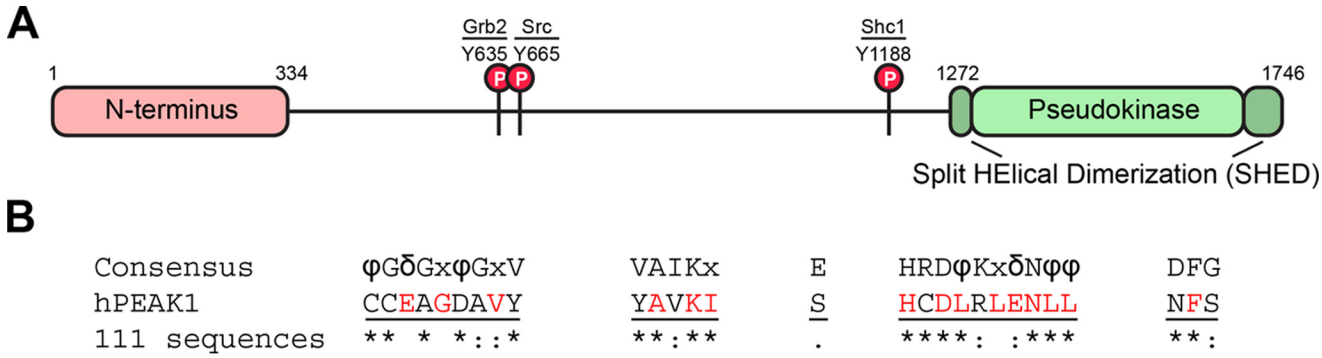

Figure 1. PEAK1 domains and kinase motifs. *A*, schematic diagram of PEAK1. Regions and domains are shown. The PEAK1 pseudokinase domain and SHED region are indicated. Some of the PEAK1 phosphorylation sites are noted, with prominent phosphotyrosine-binding proteins indicated, *e.g.* the Src SH2 binding site at Tyr^{665} (pYEEI). *B*, PEAK1 kinase motifs. *Consensus* shows consensus sequences of kinase fold motifs. δ indicates hydrophilic residue, and φ indicates hydrophobic residue. *hPEAK1* indicates sequence of human PEAK1 kinase fold motifs. Residues that strictly conform to the consensus are colored *red*. *111 sequences* indicates consensus of PEAK1 motifs across 111 sequences; *, completely conserved; :, strongly similar properties; ·, weakly similar properties by Clustal Omega (40).

(NKF3). This family consists of only two proteins, PEAK1 and pragmin (Sugen kinase 223; SgK223), which share a similar overall topology and sequence identity of over 45% between the kinase-fold domains (16, 23). On the well-known kinome phylogenetic tree (16), the NKF3 group is located proximal to the CMGC group and adjacent to the Parkinson's disease-associated kinase, PINK1. PEAK1 and pragmin are thought to contain a region N-terminal to the kinase domain that mediates both homo- and hetero-oligomerization (23); however, the role of homo-/hetero-oligomerization for PEAK1/pragmin is not well-defined. One postulation is that signaling output can be regulated by offering unique binding sites for protein interaction partners depending on the NKF3 oligomerization complex (23). These kinases therefore may harbor additional regions that mediate oligomerization events or control other aspects of signal transduction.

In this study, we determine the structure of PEAK1 pseudokinase domain and find a closed nucleotide-binding cleft. We also find that N- and C-terminal extensions together create a novel all–α-helical split dimerization region that we term the split helical dimerization (SHED) region. This represents a previously unobserved mode of kinase dimerization. PEAK1 is therefore an unusual member of the pseudokinase group.

Results

Crystal structure of PEAK1 reveals an unusual ATP-binding cleft

We crystallized PEAK1 kinase domain including both N- and C-terminal extensions but lacking the long ~40-amino acid predicted flexible loop and determined its crystal structure by molecular replacement followed by autobuilding (Fig. 2, *A–C*, and Table 1). Overall, the crystal structure illustrates that PEAK1 maintains the kinase catalytic fold with a β-sheet-rich N-lobe and an α-helical-rich C-lobe and with additional insertions (Fig. 2*D*) that are discussed below. The kinase is found in an active-like conformation, with the activation loop extended and the DFG-like motif in a DFG-in state, but no nucleotide is bound.

PEAK1 is divergent in its kinase motif conserved residues (Figs. 1*A* and 2*E*). The crystal structure shows that the glycine-rich loop (G-loop, P-loop) (conserved motif: G*X*G*XX*G) has the sequence ^{1336}CEAGDA. Secondary structure assignment in this region shows two short β-strands, termed β1′ and β1, which differs from the canonical single long β-strand, β1. The lack of glycine residues at the conserved positions suggests reduced conformational flexibility that may deleteriously impact nucleotide binding and release. This conclusion is supported in the structure where the nucleotide-binding site is closed and occluded by Tyr^{1343} (a residue that is normally a Val in competent kinases), which extends toward the predicted location of the adenine ring and hydrogen-bonds with Gln^{1388} and a water molecule. Lys^{1359} (from the conserved VAIK motif) also hydrogen bonds to Gln^{1388} and to the glycine-rich loop residue Asp^{1340}. This creates an intricate H-bonding network that appears to coordinate the glycine-rich loop to other components of the kinase fold and to be deleterious to nucleotide binding. Interestingly, there is an insert in PEAK1 between the β4 and β5 strands. Although we excised part of this loop to allow crystallization, residues 1398–1407 pack neatly against the top of the glycine-rich loop by hydrophobic interactions particularly of Trp^{1405} (Fig. 2*E*). These interactions potentially help stabilize the closed conformation of the glycine-rich loop, and Tyr^{1343} completes the formation of the hydrophobic catalytic spine, a feature of the kinase fold (24) (Fig. 2*F*).

In the PEAK1 structure, helix αC is present (residues His^{1373} to Ser^{1380}) but is flexible at its N terminus, resulting in an inability to build the model in this region. In canonical kinases, there is a glutamate residue that coordinates the VAIK lysine; however, in PEAK1 this is replaced by Ser^{1374}, which networks to Lys^{1359} via a water molecule. There are two further conserved kinase motifs. The HRD*X*K*XX*N motif is reasonably well-preserved, with a sequence of ^{1514}HCDLRLEN. However, the DFG motif is replaced with ^{1555}NFS, which suggests reduced catalytic competency (Fig. 2*E*). In sum, the kinase motif residues in PEAK1 are extensively divergent and indicate that canonical kinase activity may be lost for this pseudokinase family member. Based on the crystal structure and the closed nature of the catalytic cleft, it seems probable that the kinase is a representative of the non-nucleotide-binding class of pseudokinase.

PEAK1 dimerizes by a SHED region

The crystal structure of PEAK1 also reveals an unexpected addition to the kinase domain comprising α-helices from the

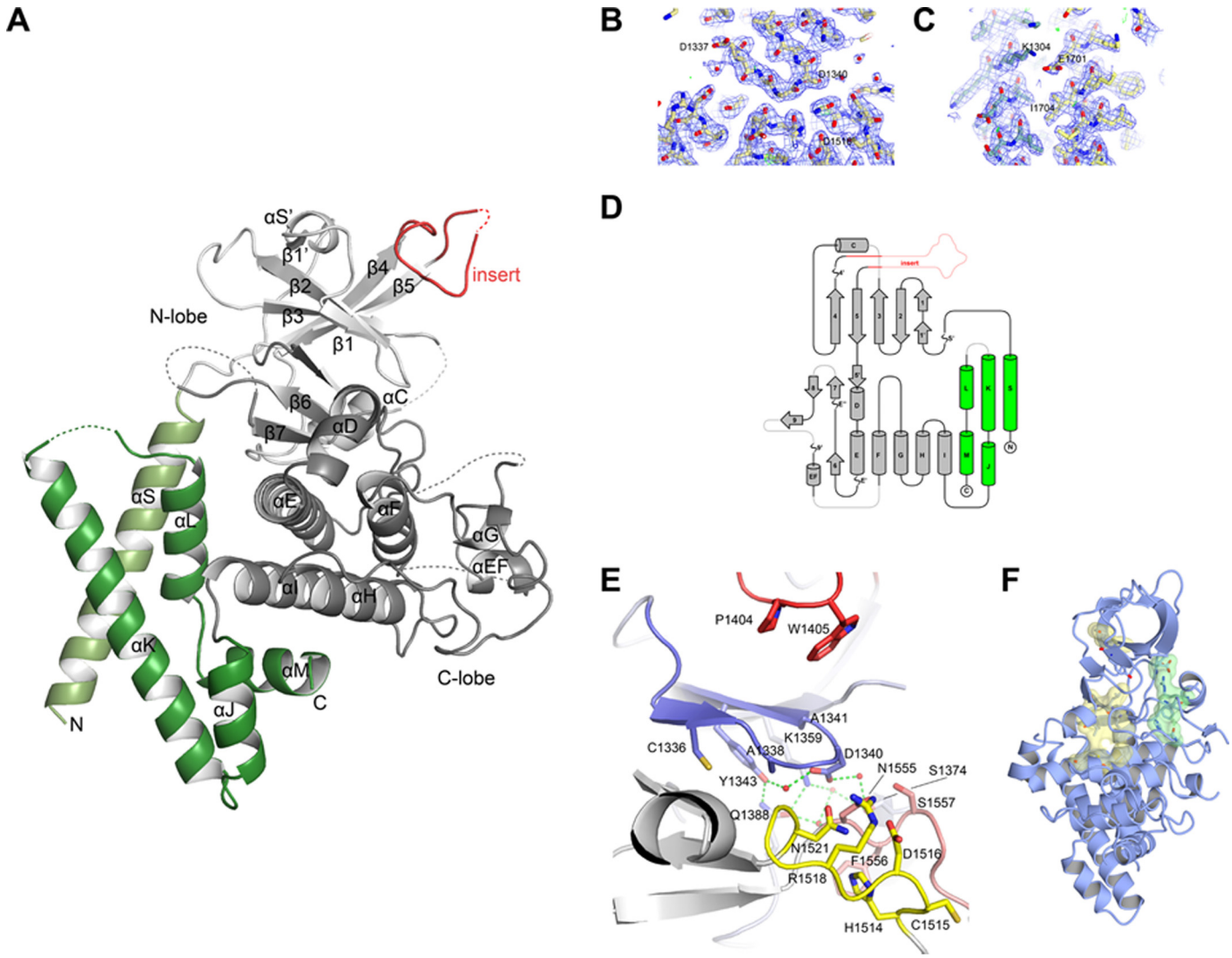

Figure 2. Structure of PEAK1 pseudokinase. *A*, structure of PEAK1 pseudokinase domain. The cartoon format is shown with the α-helices and β-strands indicated. Kinase N-lobe is colored *light gray*, and the C-lobe is in *dark gray*. The $\beta4-\beta5$ insert is shown in *red*. SHED domain colored *green*. Unmodeled loops are indicated by *dashed lines*. *B* and *C*, example electron density maps for two regions of the structure, the glycine-rich loop (*B*), and helices αS and αK (*C*). The representative residue numbers are indicated. Water molecules shown as *red spheres*. $2F_{obs} - F_{calc}$ map: *blue* shows 1σ, and *light blue* shows 2σ. In the $F_{obs} - F_{calc}$ map, *green* shows 3σ, and *red* shows -3σ. *D*, DSSP-defined (41) topology map of PEAK1 pseudokinase domain. Secondary structure elements are indicated with α-helices as *cylinders*, β-strands as *arrows*, and 3_{10} helices as *squiggles*. The SHED domain is colored *green*. $\beta4-\beta5$ insert shown in *red*. Unbuilt loops are indicated in *gray/pale red*. *E*, ATP cleft of PEAK1. Residues of the glycine-rich loop are shown in *blue*, the activation segment is in *pink* (including the DFG/NFS motif), the HRD*X*K*XX*N (HCDLRLEN) motif is in *yellow*, and the $\beta4-\beta5$ insert in *red*. Hydrogen-bonding interactions that seem to stabilize the glycine-rich loop are shown as *green dashed lines*. *F*, hydrophobic spines of PEAK1 pseudokinase domain. The regulatory spine is shaded in *green*, and the catalytic spine is in *yellow*. Tyr^{1343} completes the catalytic spine.

flanking regions both N- and C-terminal to the catalytic domain (Fig. 3*A*). One α-helix is donated to this dimerization region from residues N-terminal of the kinase domain (residues 1285–1311), and four α-helices are donated from residues C-terminal of the kinase fold (residues 1670–1743) (Fig. 2*D*). This creates an all α-helical feature that abuts the kinase C-lobe. The helices of this new region are extremely well-conserved over evolution (Fig. S1), and we term them helices αS, αJ, αK, αL, and αM. On analysis of crystal packing for PEAK1, we find a very clear dimerization interface that buries 2359 $Å^2$ (Pisa server (25)) and is mediated solely by this split domain (Fig. 3, *B* and *C*), which correlates with previous in-solution dimerization studies (23). Polar interactions are only observed between residues Glu^{1708} and Lys^{1300}, with the remainder of the large dimerization interface mediated by hydrophobic contacts (PDBsum (26)) (Fig. 3*D*), and the surface almost completely conserved over 111 species (Fig. 3*E*). We conducted extensive searches to discover whether this dimerization domain has structural homologues. The Dali server (27) suggests this arrangement to be unique, as does the VAST server (28). Therefore, we believe this to be a region that is novel among protein kinases. We term this the split helical dimerization region, or SHED region.

To biochemically validate that the SHED region mediates PEAK1 dimerization in the purified setting, we introduced a point mutation at the center of the interface, A1707D. We predicted that this mutation would disrupt dimerization by introducing a large negative charge into the hydrophobic core of the dimerization surface. Comparison of the retention of purified PEAK1 and A1707D mutant PEAK1 by size-exclu-

Table 1
Crystallographic data collection and refinement statistics

Protein	PEAK1 (sugen kinase 269, SgK269)
PDB accession code	6BHC
Data collection	
Space group	$P22_12_1$
X-ray source and detector	APS 24-ID-E, EIGER 16 M
Wavelength (Å)	0.97918
Unit cell	
a, *b*, *c* (Å)	58.9, 72.7, 103.2
α, β, γ (°)	90, 90, 90
Resolution range (Å)[a]	50.00–2.30 (2.38–2.30)
No. of unique reflections	20,320
Completeness (%)[a]	98.7 (99.1)
R_{pim} (%)[a]	8.7 (44.3)
$CC_{0.5}$ (%) (in high resolution bin)	82.3
Mean $<I>/<\sigma I>$[a]	10.1 (1.9)
Wilson *B*-factor	32.1
Redundancy	10.9 (10.6)
Refinement statistics	
Resolution range (Å)[a]	42.1–2.3 (2.42–2.3)
R_{factor} (%)[a]	19.4 (21.5)
Free R_{factor} (%)[a]	23.4 (28.9)
Free *R* reflections (%)[a]	4.8 (5.2)
Free *R* reflections (no.)[a]	955 (136)
Residues built	1285–1363, 1373–1407, 1454–1528, 1548–1562, 1572–1584, 1588–1712, 1716–1743
No. water molecules	102
Mean *B*-factor (Å^2)	
Protein	45.4
H_2O	44.2
Model statistics	
RMSD bond lengths (Å)	0.002
RMSD bond angles (°)	0.418
Ramachandran plot (favored/allowed/disallowed, %)	97.8/2.2/0

[a] High resolution shell shown in parentheses.

sion chromatography showed a significant increase in retention time for the mutant, suggesting a monomeric form compared with a dimeric wildtype PEAK1 (Fig. 3*F*).

Kinase insertions and unmodeled loops

The electron density for the crystal structure is on the whole extremely clear, allowing convincing tracing and assignment of residues directly from autobuilding. The catalytic cleft and the SHED region are both well-defined (Fig. 2, *B* and *C*); however, there are also a number of loops in the structure that have poor electron density for which we have been unable to build. In the kinase domain N-lobe, they are the β3-αC loop (residues 1364–1372) and part of the long β4–β5 insert (residues 1408–1453). In the kinase domain C-lobe, there are four unbuilt segments. They are the structurally adjacent β6-β7 (residues 1529–1547) and αK-αL loops (residues 1713–1715), portions of the activation loop (residues 1563–1571), and the αEF-αF loop (residues 1585–1587). Additionally, although we have been able to build residues of the activation segment $p + 1$ loop and αEF helix (including the APE motif), they have high *B*-factors. The connectivity of $p + 1$-αEF is ill defined, so we have built it in *cis*, as per the normal arrangement for protein kinases, adjacent to the kinase C-lobe. The PEAK1 activation segment therefore shows significant conformational flexibility.

Comparison of PEAK1 and pragmin

There are two members of the NKF3 group: PEAK1 (SgK269) and pragmin (SgK223). These proteins align with sequence identity of ~45% in the kinase domain with differences between the insertions and between the kinase motifs of PEAK1 and pragmin (Fig. 4*A*). Interestingly, pragmin is also predicted to include α-helices that comprise a SHED region. A previous study has suggested that PEAK1 and pragmin can heterodimerize (23), and based on our alignment of these proteins, there is good conservation in pragmin of SHED region residues that mediate PEAK1 homotypic dimerization (Fig. 4), indicating that homo- and heterodimerization may occur by a very similar mechanism to what we observe for PEAK1 alone. The conservation of the SHED region between PEAK1 and pragmin, and over evolution, suggests that these proteins functionally homo- and heterodimerize.

Comparison of PEAK1 and PINK1

The crystal structure of the Parkinson's disease-associated kinase, PINK1, was recently determined (29) (PDB code 5OAT). PEAK1 and PINK1 are adjacent to one another in the kinome phylogenetic tree (16). PINK1 contains multiple insertions, with one of ~30 amino acids located between strands β4 and β5 (termed Ins3 in Ref. 29). For PINK1, the Ins3 insertion seems to be important for recognition of ubiquitin as a substrate, and this insertion resembles the large PEAK1 insertion between strands β4 and β5 (Fig. 2*D*). Like PEAK1, PINK1 also contains additional helices at the C terminus of the kinase domain (termed the C-terminal extension, or CTE). This extension may be associated with homo-oligomerization and kinase catalytic activity (30), and in the PINK1 crystal structure, the CTE mediates crystallographic dimerization interactions (29). We note that the PINK1 CTE superposes extremely well with helices αJ, αK, αL, and αM of PEAK1 (Fig. 5) (RMSD, 2.3 Å over 48 aligned residues), creating a dimerization interface that resembles the PEAK1 SHED region, and that PINK1 similarly dimerizes in the symmetry lattice of its substrate-bound crystal structure (PDB code 6EQI) (31). It is therefore interesting to speculate that PINK1 may functionally dimerize through this interaction, that addition of helices equivalent to PEAK1 αS (perhaps from a binding partner) may fully recapitulate a SHED region dimerization, or that PINK1 uses its CTE to interact with an αS-like helix in binding partner proteins. Based on the structural and topographic similarities between PEAK1 and PINK1, we propose PINK1 to be the third member of the NKF3 group.

Discussion

Approximately 10% of the human kinome is comprised of pseudokinases (16). These enzymes are degraded in their conserved kinase motifs and have a variety of catalytic activities that cannot easily be predicted (18–22). The classification of protein kinases into being catalytically active, being able to bind nucleotide but harboring no catalytic activity, or being unable to bind nucleotide has helped in defining the roles of these proteins. PEAK1 (SgK269) is a member of the pseudokinase group and has been the subject of controversy surrounding its catalytic capabilities (1, 5, 9, 23); therefore structural analysis has been sought to provide a clearer picture of its functional role. The structure presented here of the kinase domain of PEAK1 allows a much-improved understanding of this unusual pseudokinase.

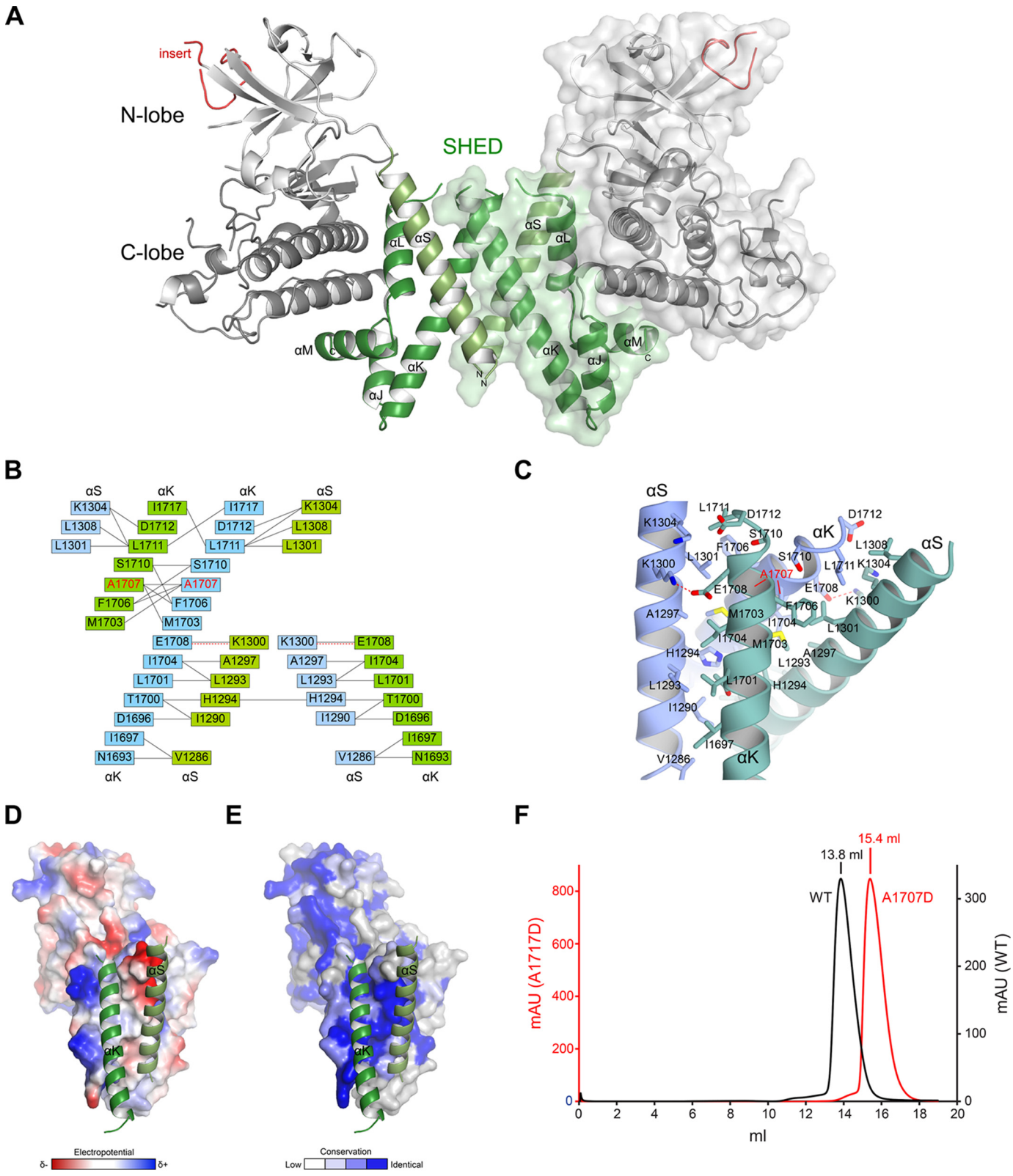

Figure 3. PEAK1 SHED region. *A*, PEAK1 homodimer. Symmetry mates shown for the PEAK1 homodimer, colored and labeled as per Fig. 2*A*. The secondary structure of the SHED region is indicated. Surface of one copy is shown. *B*, map of dimerization interactions. Electrostatic interactions are shown as *red dashed lines*, van der Waals interactions are shown as *straight lines*. The helices are indicated. Residue Ala^{1707} is indicated in *red*. *C*, close-up view of the dimerization interaction. Residues that interact are indicated. Residue Ala^{1707} is indicated in *red*. *D*, electrostatic potential of the interaction interface. Electropositive potential is shown in *blue*, and electronegative potential is in *red*. Helices αS and αK are shown in *green*. *E*, conservation of the interaction interface over 111 sequences of PEAK1. Complete conservation is shown in *blue*. Low conservation is in *white*. The results were calculated by Consurf server (42). Helices αS and αK are shown in *green*. *F*, size exclusion chromatography for wildtype and A1707D mutant PEAK1. Incorporation of the single point mutation significantly lengthens the retention time on a Superdex 200 Increase 10/300 GL (GE) column, suggesting that the A1707D mutant is a monomer.

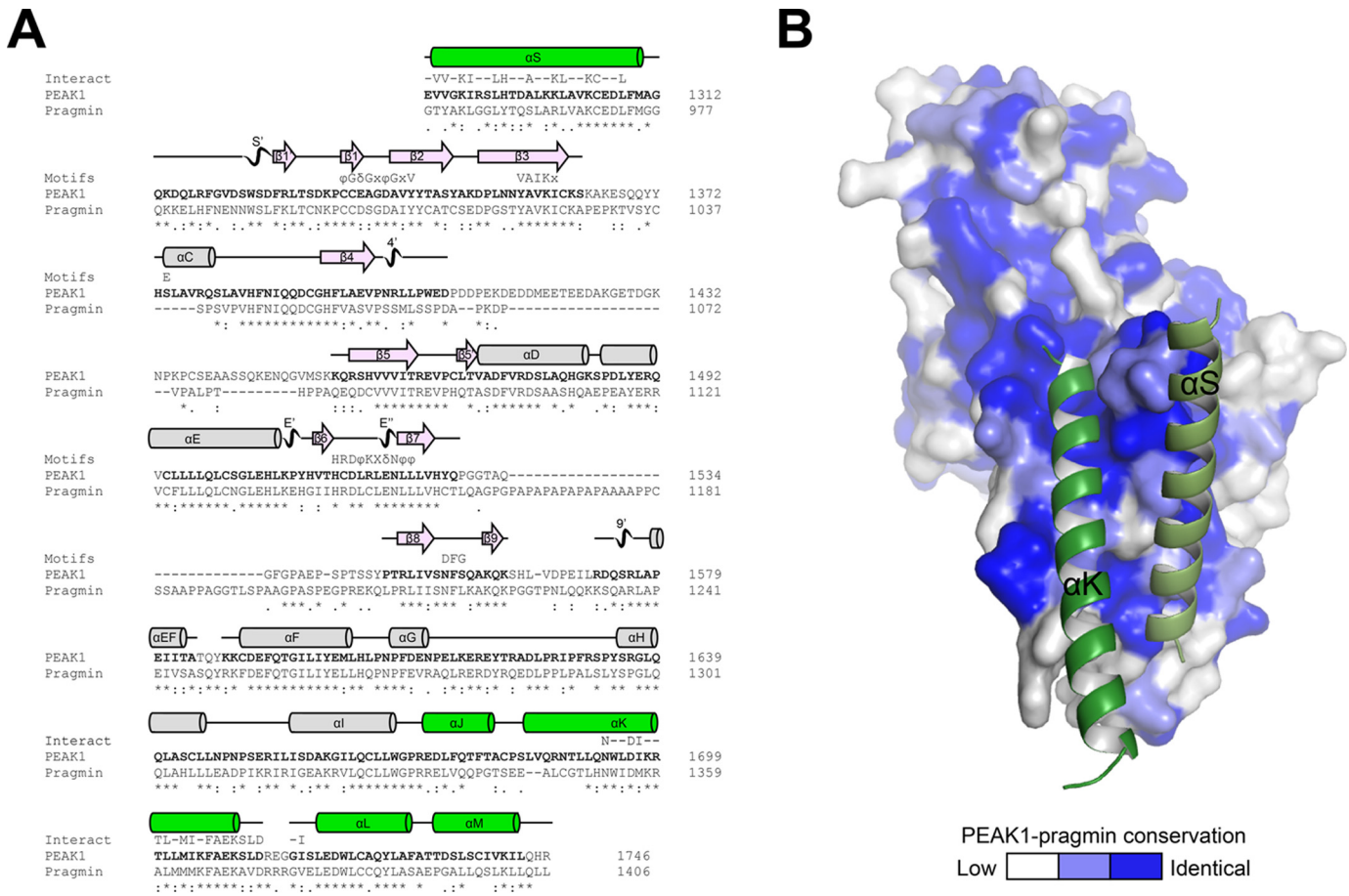

Figure 4. Comparison of PEAK1 and pragmin. *A*, alignment of PEAK1 and pragmin. DSSP-defined (41) secondary structure elements for PEAK1 are shown, with the α-helices as *cylinders*, β-strands as *arrows*, and 3_{10} helices as *squiggles*. Helices S′, 4′, and E′ are 3_{10}. Build residues of PEAK1 are in *bold type*. Conserved kinase motifs are indicated in the *Motifs* rows. Residues of PEAK1 that interact in the SHED region homodimerization interaction are indicated in the *Interact* rows. Conservation was calculated by Clustal Omega (40) and indicated as completely conserved (*), strongly similar properties (:), or weakly similar properties (·). *B*, conservation of the interaction interface between PEAK1 and pragmin. Complete conservation is shown in *blue*. Low conservation is in *white*.

In the crystal structure of PEAK1 we observe that the pseudokinase domain has a tightly closed nucleotide-binding cleft. Unusually among the kinase group, there is a tyrosine residue (Tyr^{1343}) within the glycine-rich loop that hydrogen-bonds to the C-lobe, sterically hindering nucleotide binding. This resembles the catalytic clefts of MviN and Rop2, both of which are unable to bind nucleotide because large amino acids occlude the cleft; Phe^{724}, Trp^{789}, and Tyr^{849} in MviN (32) and Tyr^{555} in Ror2 (33) (Fig. 6). Interestingly, Tyr^{1343} is in the same amino acid location as Phe^{724} from MviN, and both occlude the ATP site in a similar manner. The structure therefore indicates that that PEAK1 may fall within the "unable to bind nucleotide" class of pseudokinase and concurs with previous studies that showed its thermal stabilization upon binding Mn^{2+} but not nucleotide (18). We do not observe cation binding in the crystal structure.

The mode of dimerization for PEAK1 revealed by this crystal structure is highly unusual. The dimerization region encompasses helices both from the N and C termini of the kinase domain in a split domain configuration. We term this the SHED region and have extensively searched the databases for similar examples of this configuration. There is partial structural overlap between the SHED region (albeit without the N-terminal helix) and the CTE of the Parkinson's disease kinase, PINK1, and this similarity may indicate new modes of binding for PINK1 that have previously not been identified. Our analysis of the SHED region suggests that both homo- and heterodimerization can occur through the domain. The expression of PEAK1 is amplified in an array of cancers (including prostate, pancreatic, colon, and breast) and is associated with metastasis and proliferation (1, 4–7, 9, 12–15). These effects seem to arise from PEAK1's role as a tyrosine kinase substrate and scaffold for SH2-domain proteins such as Shc1-, Grb2-, Csk-, and Src-family kinases (4–11), and heterodimerization of PEAK1 and pragmin may play an important role in regulating these signaling cascades (23); therefore this unusual dimerization domain may represent a novel mechanism to control signaling output.

Overall, the structure of PEAK1 represents an unusual addition to the library of pseudokinase structures. Its kinase cleft is occluded, and its newly identified SHED region is unexpected and reveals a new mode of dimerization, and potentially interesting similarities that may reclassify the active kinase, PINK1, as a member of the NKF3 group.

Structure note

We note that during the final steps of manuscript preparation, a structure of pragmin (SgK223) was published (34).

Materials and methods

Expression and purification of PEAK1 kinase domain

The human PEAK1 kinase cDNA (UniProt code Q9H792) was purchased from DNASU/PSI:Biology-MR. The kinase-fold domain containing residues Gln^{1272}–Leu^{1743} with a deletion of the predicted flexible loop (ΔAsp^{1409}–Met^{1451}) was subcloned into pET-28a vector (Novagen) with an uncleavable C-terminal hexahistidine tag (LEHHHHHH). PEAK1 was expressed in BL21 (DE3)pLysS (Novagen) cells by induction with 0.5 mM isopropyl β-D-1-thiogalactopyranoside overnight at 18 °C. Harvested pellets were suspended in lysis buffer (20 mM Tris-HCl, pH 8.0, 100 mM NaCl, 1 mM tris(2-carboxyethyl)phosphine, and 0.1 mM PMSF) and lysed by sonication. The supernatants were affinity purified by HisTrap chelating column (GE) and then Resource Q (GE) ion exchange chromatography. PEAK1 was then loaded to a Superdex 200 increase 10/300 GL (GE) column. PEAK1 kinase domain eluted as monodisperse peak in 20 mM Tris-HCl, pH 8.0, 300 mM NaCl, and 1 mM tris(2-carboxyethyl)phosphine. Mutations were introduced using the QuikChange (Agilent Technologies), and protein was purified identically to wildtype.

Crystallization and data collection

PEAK1 kinase domain was concentrated to 0.8 mg/ml for crystal trials and mixed with 0.5 mM staurosporine dissolved in DMSO prior to setting up crystallization drops. Following overnight incubation of PEAK1 kinase domain and staurosporine, the complex was centrifuged, and the supernatants were used for crystal screening. Initial crystallization screening was performed using the sitting-drop method with a TTP Labtech Mosquito crystallization robot. Initial crystals were observed after a week at room temperature against precipitant conditions of 100 mM HEPES, pH 6.5, and 10% (v/v) PEG 6000. For data collection, crystals were screened with various buffers, pH, and PEGs, and optimal conditions were found to be 100 mM *N*-(2-acetamido) iminodiacetic acid, pH 6.8, and 11% (v/v) PEG 3350. The largest crystals in these conditions grew to dimensions of 35 × 35 × 2 μm. Crystals were cryoprotected in reservoir buffer supplemented with 35% (v/v) ethylene glycerol.

Structure determination and refinement

Crystallographic data were processed to 2.3 Å resolution using the HKL2000 package (36) for a data set from a single crystal. 180° of data in 0.5° oscillations were collected at the Advanced Photon Source Beamline 24-ID-E, which was equipped with a Dectris EIGER 16M detector. Based on Matthews coefficient analysis, we expected one molecule per asymmetric unit. We conducted multiple attempts at structure determination using molecular replacement and automatic model building but found that although we could consistently obtain an initial solution for the kinase C-lobe (Phaser TFZ-scores over 7), the models were too poor to achieve a full structure solution. Following extensive trials, we finally determined the structure using the BALBES automatic molecular replacement pipeline (37), which gave an initial solution with tailored human Nek 7 (PDB code 2WQM) as the search model, and we input this model into ARP/wARP. Multiple runs of ARP/wARP (web-based version 7.6) were conducted using varying sigma cutoff levels for addition of new atoms. The best result from each round was input again to ARP/wARP. In total, over 400

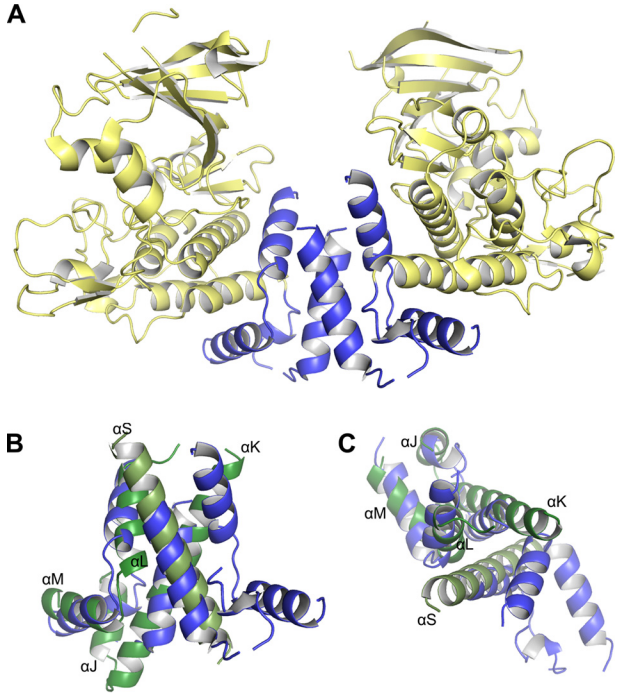

Figure 5. Comparison of the structures PEAK1 and PINK1. *A*, structure of PINK1 (PDB code 5OAT) (29) showing crystallographic CTE–mediated dimerization via a symmetry mate. Kinase domains are in *yellow*, and CTEs are in *blue*. *B*, superposition of PINK1 CTE and one-half of the PEAK1 SHED region illustrating the similarity of the regions. The helices of PEAK1 are indicated and shown in *green*. *C*, top view of superposed PINK1 CTE and one-half of the PEAK1 SHED region.

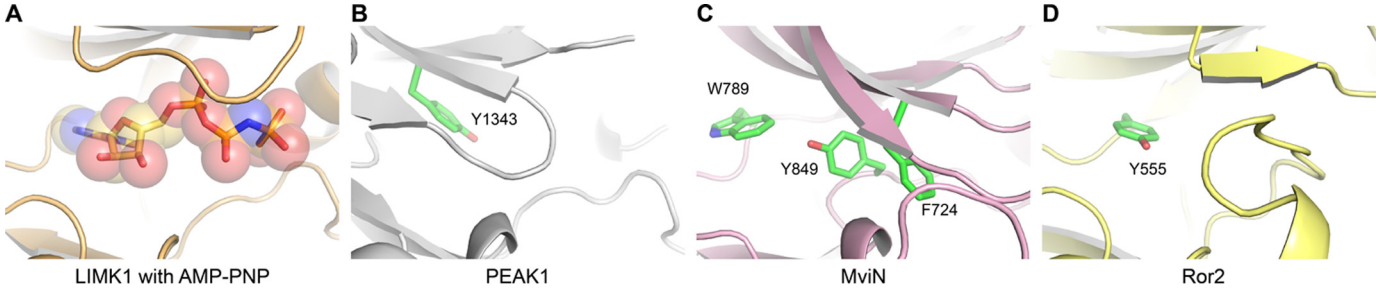

Figure 6. Occlusion of ATP-binding clefts in pseudokinases. *A*, example of an active LIMK1 bound to ATP analogue AMP-PNP (PDB code 5HVK; Ref. 43). *B*, PEAK1 showing Tyr^{1343} in the ATP-binding cleft. *C*, MviN pseudokinase showing residues Phe^{724}, Trp^{789}, and Tyr^{849} occluding the ATP binding cleft (PDB code 3OTV; Ref. 32). *D*, Ror2 showing Tyr^{555} occluding the ATP-binding cleft (PDB code 4GT4; Ref. .33). Structures are superposed on the C-lobes to show the same orientation.

separate runs of ARP/wARP were conducted, allowing the structure to be determined with 365 residues of PEAK1 autobuilt, containing 85% of the sequence. The final ARP/wARP solution yielded R/R_{free} of 26.0%/30.9% following refinement in Phenix refine (38). Manual model building was then carried out in Coot (39) and refined in Phenix including TLS parameters. Good electron density is observed throughout the model, but some loops are flexible, allowing us to build the following residues of PEAK1: 1285–1363, 1373–1407, 1454–1528, 1548–1562, 1572–1584, 1588–1712, and 1716–1743. No density for staurosporine is visible. The final overall structure of PEAK1 is most similar to RET receptor tyrosine kinase (Dali server, RMSD 2.7 Å over 232 residues, 19% identity, Dali *Z* score 22.3; PDB code 2X2L) and Aurora A serine/threonine kinase (Dali server, RMSD 2.6 Å over 229 residues, 24% identity, Dali *Z* score 22.3; PDB code 3D14).

Author contributions—B. H. H. data curation; B. H. H. formal analysis; B. H. H. and T. J. B. validation; B. H. H. investigation; B. H. H. and T. J. B. visualization; B. H. H. and T. J. B. methodology; B. H. H. and T. J. B. writing-original draft; B. H. H. and T. J. B. writing-review and editing; T. J. B. conceptualization; T. J. B. supervision; T. J. B. funding acquisition; T. J. B. project administration.

Acknowledgments—We thank Ben Turk, Mark Lemmon, and Amy Stiegler. We also thank Advanced Photon Source Beamline NE-CAT (24-ID-E and -C). The Advanced Photon Source Beamline NE-CAT 24-ID-E and -C was supported in part by National Institutes of Health Grants GM103403 and RR029205.

References

1. Wang, Y., Kelber, J. A., Tran Cao, H. S., Cantin, G. T., Lin, R., Wang, W., Kaushal, S., Bristow, J. M., Edgington, T. S., Hoffman, R. M., Bouvet, M., Yates J. R., 3rd, and Klemke, R. L. (2010) Pseudopodium-enriched atypical kinase 1 regulates the cytoskeleton and cancer progression [corrected]. *Proc. Natl. Acad. Sci. U.S.A.* **107,** 10920–10925 CrossRef Medline
2. Kelber, J. A., and Klemke, R. L. (2010) PEAK1, a novel kinase target in the fight against cancer. *Oncotarget* **1,** 219–223 CrossRef Medline
3. Ohara, O., Nagase, T., Mitsui, G., Kohga, H., Kikuno, R., Hiraoka, S., Takahashi, Y., Kitajima, S., Saga, Y., and Koseki, H. (2002) Characterization of size-fractionated cDNA libraries generated by the in vitro recombination-assisted method. *DNA Res.* **9,** 47–57 CrossRef Medline
4. Zheng, Y., Zhang, C., Croucher, D. R., Soliman, M. A., St-Denis, N., Pasculescu, A., Taylor, L., Tate, S. A., Hardy, W. R., Colwill, K., Dai, A. Y., Bagshaw, R., Dennis, J. W., Gingras, A. C., Daly, R. J., *et al.* (2013) Temporal regulation of EGF signalling networks by the scaffold protein Shc1. *Nature* **499,** 166–171 CrossRef Medline
5. Kelber, J. A., Reno, T., Kaushal, S., Metildi, C., Wright, T., Stoletov, K., Weems, J. M., Park, F. D., Mose, E., Wang, Y., Hoffman, R. M., Lowy, A. M., Bouvet, M., and Klemke, R. L. (2012) KRas induces a Src/PEAK1/ErbB2 kinase amplification loop that drives metastatic growth and therapy resistance in pancreatic cancer. *Cancer Res.* **72,** 2554–2564 CrossRef Medline
6. Croucher, D. R., Hochgräfe, F., Zhang, L., Liu, L., Lyons, R. J., Rickwood, D., Tactacan, C. M., Browne, B. C., Ali, N., Chan, H., Shearer, R., Gallego-Ortega, D., Saunders, D. N., Swarbrick, A., and Daly, R. J. (2013) Involvement of Lyn and the atypical kinase SgK269/PEAK1 in a basal breast cancer signaling pathway. *Cancer Res.* **73,** 1969–1980 CrossRef Medline
7. Leroy, C., Fialin, C., Sirvent, A., Simon, V., Urbach, S., Poncet, J., Robert, B., Jouin, P., and Roche, S. (2009) Quantitative phosphoproteomics reveals a cluster of tyrosine kinases that mediates SRC invasive activity in advanced colon carcinoma cells. *Cancer Res.* **69,** 2279–2286 CrossRef Medline
8. Titz, B., Low, T., Komisopoulou, E., Chen, S. S., Rubbi, L., and Graeber, T. G. (2010) The proximal signaling network of the BCR-ABL1 oncogene shows a modular organization. *Oncogene* **29,** 5895–5910 CrossRef Medline
9. Tactacan, C. M., Phua, Y. W., Liu, L., Zhang, L., Humphrey, E. S., Cowley, M., Pinese, M., Biankin, A. V., and Daly, R. J. (2015) The pseudokinase SgK223 promotes invasion of pancreatic ductal epithelial cells through JAK1/Stat3 signaling. *Mol. Cancer* **14,** 139 CrossRef Medline
10. Bristow, J. M., Reno, T. A., Jo, M., Gonias, S. L., and Klemke, R. L. (2013) Dynamic phosphorylation of tyrosine 665 in pseudopodium-enriched atypical kinase 1 (PEAK1) is essential for the regulation of cell migration and focal adhesion turnover. *J. Biol. Chem.* **288,** 123–131 CrossRef Medline
11. Hochgräfe, F., Zhang, L., O'Toole, S. A., Browne, B. C., Pinese, M., Porta Cubas, A., Lehrbach, G. M., Croucher, D. R., Rickwood, D., Boulghourjian, A., Shearer, R., Nair, R., Swarbrick, A., Faratian, D., Mullen, P., *et al.* (2010) Tyrosine phosphorylation profiling reveals the signaling network characteristics of basal breast cancer cells. *Cancer Res.* **70,** 9391–9401 CrossRef Medline
12. Fujimura, K., Wright, T., Strnadel, J., Kaushal, S., Metildi, C., Lowy, A. M., Bouvet, M., Kelber, J. A., and Klemke, R. L. (2014) A hypusine-eIF5A-PEAK1 switch regulates the pathogenesis of pancreatic cancer. *Cancer Res.* **74,** 6671–6681 CrossRef Medline
13. Strnadel, J., Choi, S., Fujimura, K., Wang, H., Zhang, W., Wyse, M., Wright, T., Gross, E., Peinado, C., Park, H. W., Bui, J., Kelber, J., Bouvet, M., Guan, K. L., and Klemke, R. L. (2017) eIF5A-PEAK1 signaling regulates YAP1/TAZ protein expression and pancreatic cancer cell growth. *Cancer Res.* **77,** 1997–2007 CrossRef Medline
14. Agajanian, M., Runa, F., and Kelber, J. A. (2015) Identification of a PEAK1/ZEB1 signaling axis during TGFβ/fibronectin-induced EMT in breast cancer. *Biochem. Biophys. Res. Commun.* **465,** 606–612 CrossRef Medline
15. Agajanian, M., Campeau, A., Hoover, M., Hou, A., Brambilla, D., Kim, S. L., Klemke, R. L., and Kelber, J. A. (2015) PEAK1 acts as a molecular switch to regulate context-dependent TGFβ responses in breast cancer. *PLoS One* **10,** e0135748 CrossRef Medline
16. Manning, G., Whyte, D. B., Martinez, R., Hunter, T., and Sudarsanam, S. (2002) The protein kinase complement of the human genome. *Science* **298,** 1912–1934 CrossRef Medline
17. Boudeau, J., Miranda-Saavedra, D., Barton, G. J., and Alessi, D. R. (2006) Emerging roles of pseudokinases. *Trends Cell Biol.* **16,** 443–452 CrossRef Medline
18. Murphy, J. M., Zhang, Q., Young, S. N., Reese, M. L., Bailey, F. P., Eyers, P. A., Ungureanu, D., Hammaren, H., Silvennoinen, O., Varghese, L. N., Chen, K., Tripaydonis, A., Jura, N., Fukuda, K., Qin, J., *et al.* (2014) A robust methodology to subclassify pseudokinases based on their nucleotide-binding properties. *Biochem. J.* **457,** 323–334 CrossRef Medline
19. Murphy, J. M., Mace, P. D., and Eyers, P. A. (2017) Live and let die: insights into pseudoenzyme mechanisms from structure. *Curr. Opin. Struct. Biol.* **47,** 95–104 CrossRef Medline
20. Stiegler, A. L., and Boggon, T. J. (2017) p190RhoGAP proteins contain pseudoGTPase domains. *Nat. Commun.* **8,** 506 CrossRef Medline
21. Zeqiraj, E., and van Aalten, D. M. (2010) Pseudokinases-remnants of evolution or key allosteric regulators? *Curr. Opin. Struct. Biol.* **20,** 772–781 CrossRef Medline
22. Hammarén, H. M., Virtanen, A. T., and Silvennoinen, O. (2015) Nucleotide-binding mechanisms in pseudokinases. *Biosci. Rep.* **36,** e00282 Medline
23. Liu, L., Phua, Y. W., Lee, R. S., Ma, X., Jenkins, Y., Novy, K., Humphrey, E. S., Chan, H., Shearer, R., Ong, P. C., Dai, W., Saunders, D. N., Lucet, I. S., and Daly, R. J. (2016) Homo- and heterotypic association regulates signaling by the SgK269/PEAK1 and SgK223 pseudokinases. *J. Biol. Chem.* **291,** 21571–21583 CrossRef Medline
24. Kornev, A. P., Haste, N. M., Taylor, S. S., and Eyck, L. F. (2006) Surface comparison of active and inactive protein kinases identifies a conserved activation mechanism. *Proc. Natl. Acad. Sci. U.S.A.* **103,** 17783–17788 CrossRef Medline
25. Krissinel, E., and Henrick, K. (2007) Inference of macromolecular assemblies from crystalline state. *J. Mol. Biol.* **372,** 774–797 CrossRef Medline

26. Laskowski, R. A. (2009) PDBsum new things. *Nucleic Acids Res.* **37,** D355–D359 CrossRef Medline
27. Holm, L., and Sander, C. (1997) Dali/FSSP classification of three-dimensional protein folds. *Nucleic Acids Res.* **25,** 231–234 CrossRef Medline
28. Gibrat, J. F., Madej, T., and Bryant, S. H. (1996) Surprising similarities in structure comparison. *Curr. Opin Struct. Biol.* **6,** 377–385 CrossRef Medline
29. Kumar, A., Tamjar, J., Waddell, A. D., Woodroof, H. I., Raimi, O. G., Shaw, A. M., Peggie, M., Muqit, M. M., and van Aalten, D. M. (2017) Structure of PINK1 and mechanisms of Parkinson's disease associated mutations. *Elife* **6,** e29985 Medline
30. Okatsu, K., Uno, M., Koyano, F., Go, E., Kimura, M., Oka, T., Tanaka, K., and Matsuda, N. (2013) A dimeric PINK1-containing complex on depolarized mitochondria stimulates Parkin recruitment. *J. Biol. Chem.* **288,** 36372–36384 CrossRef Medline
31. Schubert, A. F., Gladkova, C., Pardon, E., Wagstaff, J. L., Freund, S. M. V., Steyaert, J., Maslen, S. L., and Komander, D. (2017) Structure of PINK1 in complex with its substrate ubiquitin. *Nature* **552,** 51–56 CrossRef Medline
32. Gee, C. L., Papavinasasundaram, K. G., Blair, S. R., Baer, C. E., Falick, A. M., King, D. S., Griffin, J. E., Venghatakrishnan, H., Zukauskas, A., Wei, J. R., Dhiman, R. K., Crick, D. C., Rubin, E. J., Sassetti, C. M., and Alber, T. (2012) A phosphorylated pseudokinase complex controls cell wall synthesis in mycobacteria. *Sci. Signal.* **5,** ra7 Medline
33. Artim, S. C., Mendrola, J. M., and Lemmon, M. A. (2012) Assessing the range of kinase autoinhibition mechanisms in the insulin receptor family. *Biochem. J.* **448,** 213–220 CrossRef Medline
34. Patel, O., Griffin, M. D. W., Panjikar, S., Dai, W., Ma, X., Chan, H., Zheng, C., Kropp, A., Murphy, J. M., Daly, R. J., and Lucet, I. S. (2017) Structure of SgK223 pseudokinase reveals novel mechanisms of homotypic and heterotypic association. *Nat. Commun.* **8,** 1157 CrossRef Medline
35. Meyer, P. A., Socias, S., Key, J., Ransey, E., Tjon, E. C., Buschiazzo, A., Lei, M., Botka, C., Withrow, J., Neau, D., Rajashankar, K., Anderson, K. S., Baxter, R. H., Blacklow, S. C., Boggon, T. J., *et al.* (2016) Data publication with the structural biology data grid supports live analysis. *Nat. Commun.* **7,** 10882 CrossRef Medline
36. Otwinowski, Z., and Minor, W. (1997) Processing of X-ray diffraction data collected in oscillation mode. *Methods Enzymol.* **276**, 307–326 CrossRef Medline
37. Long, F., Vagin, A. A., Young, P., and Murshudov, G. N. (2008) BALBES: a molecular-replacement pipeline. *Acta Crystallogr. D Biol. Crystallogr.* **64,** 125–132 CrossRef Medline
38. Adams, P. D., Afonine, P. V., Bunkóczi, G., Chen, V. B., Davis, I. W., Echols, N., Headd, J. J., Hung, L. W., Kapral, G. J., Grosse-Kunstleve, R. W., McCoy, A. J., Moriarty, N. W., Oeffner, R., Read, R. J., Richardson, D. C., *et al.* (2010) PHENIX: a comprehensive Python-based system for macromolecular structure solution. *Acta Crystallogr. D Biol. Crystallogr.* **66,** 213–221 CrossRef Medline
39. Emsley, P., Lohkamp, B., Scott, W. G., and Cowtan, K. (2010) Features and development of Coot. *Acta Crystallogr. D Biol. Crystallogr.* **66,** 486–501 CrossRef Medline
40. Sievers, F., Wilm, A., Dineen, D., Gibson, T. J., Karplus, K., Li, W., Lopez, R., McWilliam, H., Remmert, M., Söding, J., Thompson, J. D., and Higgins, D. G. (2011) Fast, scalable generation of high-quality protein multiple sequence alignments using Clustal Omega. *Mol. Syst Biol.* **7,** 539 Medline
41. Kabsch, W., and Sander, C. (1983) Dictionary of protein secondary structure: pattern recognition of hydrogen-bonded and geometrical features. *Biopolymers* **22,** 2577–2637 CrossRef Medline
42. Landau, M., Mayrose, I., Rosenberg, Y., Glaser, F., Martz, E., Pupko, T., and Ben-Tal, N. (2005) ConSurf 2005: the projection of evolutionary conservation scores of residues on protein structures. *Nucleic Acids Res.* **33,** W299–W302 CrossRef Medline
43. Hamill, S., Lou, H. J., Turk, B. E., and Boggon, T. J. (2016) Structural basis for non-canonical substrate recognition of cofilin/ADF proteins by LIM kinases. *Mol. Cell* **62,** 397–408 CrossRef Medline